


Preliminary Design of “Baseline-II” Blended Wing-Body (BWB) Unmanned Aerial Vehicle (UAV): Achieving Higher Aero...

Wahyu Kuntjoro, Rizal Nasir, Wirachman Wisnoe, Zurriati Ali

Related papers

[Download a PDF Pack](#) of the best related papers 



[Aerodynamic, Stability and Flying Quality Evaluation on a Small Blended Wing-body Aircraft wit...](#)

Wahyu Kuntjoro, Wirachman Wisnoe

[Experimental results analysis for UiT M BWB baseline-I and baseline-II UAV running at 0.1 mach number](#)

Wirachman Wisnoe

[Aerodynamic Shape Optimization of a Blended-Wing-Body Aircraft Configuration](#)

Divakar Mohanraj

Preliminary Design of “Baseline-II” Blended Wing-Body (BWB) Unmanned Aerial Vehicle (UAV): Achieving Higher Aerodynamic Efficiency Through Planform Redesign and Low-Fidelity Inverse Twist Method

Rizal E. M. Nasir, Wahyu Kuntjoro, Wirachman Wisnoe, Zurriati Ali, Nor F. Reduan, Firdaus Mohamad, Shahrizal Suboh

Abstract— The purposes of proposing blended wing-body aircrafts (BWB) as replacement to conventionally-designed aircrafts for air transport purposes are to take advantage on increasing lift force due to larger effective lifting area per wing span and reducing drag force due to smaller interference drag, hence, improving aerodynamic efficiency that leads to lesser thrust required for the same flight mission weight and lower fuel consumption. The case study presented here is a proposed BWB design for unmanned aerial vehicle (UAV) known as “Baseline-II” that is actually a completely-revised, redesigned version of “Baseline-I” BWB (also known as HANTU). The Baseline-II features simpler planform, broader-chord wing and slimmer body than its predecessor while maintaining wing span. The objective is to improve flight performance at low cruising speed by increasing lift-to-drag ratio through planform redesign and inverse twist method on airfoils throughout its span. Low-fidelity aerodynamic computation with simplification to computation model is made at this stage to reduce design time. Baseline-I’s large centre elevator is replaced by smaller canard to achieve sufficient longitudinal stability while increasing lift as opposed to the former which degrades lift during flight. The result is that Baseline-II achieves higher aerodynamic efficiency (lift-to-drag ratio) and it is able to cruise at lower airspeed with lower thrust required than Baseline-I.

Keywords: Aerodynamics, Blended Wing-Body, Unmanned Aerial Vehicle, Aircraft Design

Rizal E. M. Nasir is with the Flight Technology & Testing Centre (FTTC), Faculty of Mechanical Engineering, Universiti Teknologi MARA, 40450 Shah Alam, Malaysia. He is currently conducting Ph.D. research in flight dynamics of blended wing-body aircraft (Tel: +60-3-55436207; Fax: +60-3-55435160; Email: fendy117@gmail.com, rizal524@salam.uitm.edu.my).

Dr. Wahyu Kuntjoro is a professor at the Flight Technology & Testing Centre (FTTC). His research focus includes aircraft structural integrity, aircraft design and dynamics (Email: wkuntjoro@yahoo.com).

Dr. Wirachman Wisnoe is an associate professor at the Flight Technology & Testing Centre (FTTC). His research focuses on aerodynamics (Email: wira_wisnoe@yahoo.com).

Zurriati Ali is with the Flight Technology & Testing Centre (FTTC). She is currently conducting Ph.D. research in aerodynamics (Email: zurrie_adik@gmail.com). Nor F. Reduan and Firdaus Mohamad are MSc. Research students in aerodynamics. Shahrizal Suboh is a wind tunnel technician at FTTC.

I. INTRODUCTION

Blended wing-body (BWB) configuration is expected to replace conventional fuselage-wing-tail configuration as the next airliners and transport aircrafts. It is a hybrid of flying-wing (all-wing configuration) and conventional aircraft [1]. The purposes of BWB configurations are many; some of them are to increase lift force due to larger effective lifting area per wing span [2] and reducing drag by minimizing interference drag [3]. BWB aircraft also has better flight stability characteristic than the flying-wing aircraft [4] that is known for tumbling problem [5]-[6].

As a result of lift increase and drag reduction, the lift-to-drag ratio (L/D) of BWB is higher than the current conventional airliners thus reducing fuel consumption up to 30 percent [1]. Many researchers have confirmed the claim such as Qin et. al. with $L/D = 25$ for 450-seat BWB [7], Zhu et. al. with $L/D = 23$ for 800-seat BWB [8] and other similar values observed by similar L/D improvements are observed by Portsdam et. al. [9], Katz et. al. [10], Wakayama and Kroo [11], Bolsunovsky et. al. [12], Roman et. al. [13], Österheld et. al. [3], Engels et. al. [2] and Liebeck [13]. L/D for Airbus A380 is 19 and many other airliners have L/D ranging from 15 to 20. Higher L/D means lower thrust required to propel an aircraft at design cruising speed [1].

The case study presented here is a proposed BWB design for unmanned aerial vehicle (UAV) known as “Baseline-II” that is actually a completely-revised, redesigned version of “Baseline-I” BWB (also known as HANTU) [14]. Baseline-I BWB is a four-metre span mini UAV class of aircraft with MTOW of 200 kg that shall loiter at its design airspeed of Mach 0.1. The Baseline-II features simpler planform, broader-chord wing and slimmer body than its predecessor while maintaining wing span. The objective is to improve flight performance at low cruising speed by increasing lift-to-drag ratio through planform and shape redesign, and inverse twist method on airfoils throughout its span.

II. LESSONS LEARNED FROM BASELINE-I DESIGN

Aerodynamic nature of BWB aircraft is non-linear as observed by 100-seat lifting-body aircraft by Katz et. al. [10], and wide-body BWB airliners (more than 400 seat) by Wakayama and Kroo [11], Roman et. al. [13], Österheld et. al. [3], Engels et. al. [2], de Castro [15], Qin et. al. [7] – by computational (CFD) or/and wind tunnel experiments. Similar trend was observed on Baseline-I BWB (Figure 1) by Wisnoe et. al. [16], Mamat et. al. [14] and Nasir et. al. [17],[19]. All observed wing stall at low-to-mid angles of attack while the body continues to generate lift at high incidence angles via leading edge vortex lift. Cummings et. al. [18] also observes similar phenomenon of vortex lift on the body of BWB UAV. Stall angle of attack (incidence angle) is found at 40 deg while UiTM's Baseline-I stall angle was 35 deg.

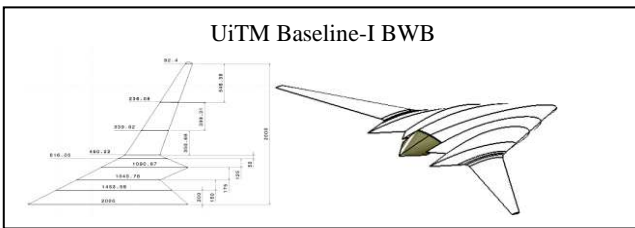


Figure 1: UiTM Baseline-I BWB

Computational aerodynamics simulation and wind tunnel tests for Baseline-I looks promising as it has high incidence angle capability that enables shorter landing distance, however, there are many shortcomings of this design;

1. The change of lift coefficient C_L with respect to incidence angle α is low – the value of C_L is small and inadequate to fly at loitering/design airspeed of Mach 0.1 if one were to set its trim angle at low α . It needs to fly at Mach 0.3-0.35 for optimum airspeed at $MTOW$ and Mach 0.17 at 100-kg weight [14],[17]-[19]. Loss of lift happens on the wing at low incidence angle - eight degrees to be specific. The wing is also very small (area) compares with its body.
2. The maximum lift coefficient $C_{L_{max}}$ is low at 1.02 – 1.15 using computational simulation [14],[17],[19] and even lower at 0.70 tested in wind tunnel at Mach 0.1 [18]. The stall speed is high and low-speed landing approach is impossible.
3. Minimum drag varies from 0.0156-0.0215 from computational aerodynamics to 0.025 from wind tunnel test [14],[17]-[19]. Due to sharp edges and radical change of sweep angle between body and wing, the interference drag is high. Induce drag is also high due to low aerodynamic efficiency (Oswald's efficiency). Although the body also generates lift, it is of delta shape that has very thick section (up to 22 percent chord) and its width is 32 percent of total aircraft span that produces tremendous profile drag.
4. Low L/D is observed – from 9 to 14 from computational aerodynamics to only 8 from wind tunnel test [14],[17]-[19]. The body has to trim at seven degrees of incidence to achieve the best L/D – an angle very close to condition where the lost of lift on the wing begins.

5. Computational aerodynamics shows that local lift loading $C_{lc}/(MAC)$ along spanwise station from centre body to wing tip is not elliptical, hence not optimum to produce high L/D [14].
6. The centre body elevator located aft of the body is ineffective as the pitching moment produced is very high causing change of trim impossible [17]. This is due to separations and unpredictable turbulence at aft of the body.

III. MODIFICATIONS TO PLANFORM AND SHAPE

It is decided that the planform of the BWB Baseline-I shall be modified. The modification is extensive that it has evolved into a new design known as Baseline-II. The wing span, body length and reference planform area are similar to Baseline-I. Baseline-II's $MTOW$ is reduced to 100 to 130 kg due to lighter electronic components, extensive use of composite material and plastics instead of aluminium, smaller engine size and weight, and lesser fuel capacity (with the same range capability). Baseline-I's $MTOW$ is also updated to within the same weight region due to the same reasons. Then, modifications to the planform and shape are executed to solve shortcomings of Baseline-I.

Mod 1 – Frontal view area of the aircraft is changed from 32-percent body span (to incorporate twin engine inside) to 15-percent body span (only single engine inside) resulting in thinner body and longer wing. The modification is based on recommendation by Bolsunovsky [5]. This modification is to address shortcomings 1 - small wing area and 3 - high profile drag. The frontal view profile is generated using mathematical equations divided into three regions; body, wing-body (outer body in Baseline-I) and wing. Mid-wing configuration is changed to high-wing configuration for lateral stability reasons.

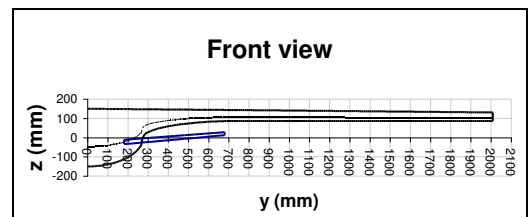


Figure 2: Front view of Baseline-II (half span)

Mod 2 – The wing and body airfoil sections are changed to simpler but high-lift form while maintaining 12 to 15 percent thickness-to-chord ratio (t/c). Instead of adjusting thickness to suit the planform in Baseline-I (causing t/c to soar up to 22 percent at certain spanwise station), Baseline-II design process adjusts planform (by adjusting chord length and longitudinal location) to suit to the thickness of spanwise station. Once again, mathematical model of this planform is generated and divided into three regions mentioned in Mod 1. No more sharp edges are incorporated on any part of the wing-body. Instead, the transition from body to wing is smooth. Mod 2 purpose is to solve Baseline-I's shortcomings no 1 – low C_L w.r.t. α and small wing

area, 2 – low $C_{L_{\max}}$ hence high stall speed, and 3 – high interference drag and high profile drag. Installation of canard foreplanes is to solve shortcoming 6 – trim problem and flight longitudinal stability (will not be discussed further), and can help by increasing lift coefficient. There will be some interference drag due to body-canard attachment and downwash to the wing-body region behind the canard but they are assumed to give smaller effect to the rise of drag than the benefit coming from lift increase.

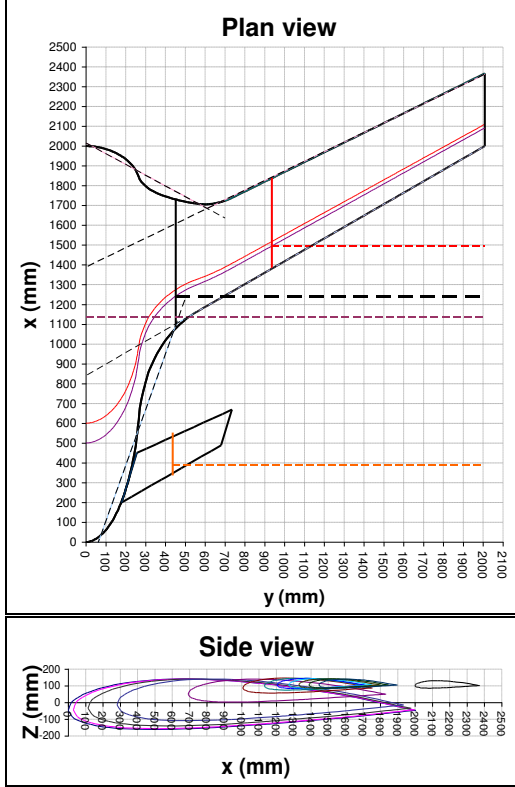


Figure 3: Plan view (half span) and side view showing wing-body airfoil profiles.

Mod 3 – The wing and canard are swept 30 degrees back for better high-speed performance, trim angle and longitudinal stability as recommended by Siouris and Qin [20]. In the context of this paper, Mod 3 is conducted to solve shortcoming 6.

Figure 2 and 3 become the basis of three-dimensional model of Baseline-II BWB. Baseline-I's shortcoming 3 – high induced drag, 4 and 5 will be solved using low-fidelity inverse twist design.

IV. LOW-FIDELITY INVERSE TWIST

BWB, since its body also generates lift, has quite an unconventional lift loading. Unlike conventional fuselage-wing-tail configuration where the wing is the main contributor to lift generation, BWB has large amount of lift generated by its body and this is actually the purpose of BWB – to generate lift on all surfaces. Wing loading or local lift loading on spanwise location (ΔC_{Li}) is a function of angle of section (local airfoil) lift coefficient (C_{li}), local chord (c_i) and mean aerodynamic chord (MAC);

$$\Delta C_{Li} = C_{li}c_i / (MAC)$$

Optimization of wing loading using inverse twist method suggests that a sectional lift coefficient C_{li} is obtained first via computational simulation and then local lift loading is calculated. The summation of local lift throughout the span (the area under lift loading curve) is computed to obtain total lift coefficient of the aircraft, C_L . A mathematical equation is derived for an ideal local lift loading as functions of spanwise location and total lift coefficient of aircraft. Finally, the incidence angle of local airfoil section is changed (in other words, is twisted) to suit to ideal local lift loading. This process is known as inverse twist – it is the inverse process of normal aircraft design process where the wing is twisted first to analyze its lift loading. Many studies resort to this method or derivative of similar method for obtaining the best lift loading at design incidence angle to achieve the best L/D such as in [2],[3],[7],[11].

However, prediction of sectional lift coefficient in three-dimensional world is easier said than done, plus it is very time-consuming and expensive. Sectional lift coefficient is not just a function of incidence angle and airfoil's mathematical characteristic but also a function of many other factor and flow coming from neighboring sections. A low-fidelity inverse-twist method is proposed here to simplify the design process. Assuming that BWB aircraft is made of a large but finite number of airfoil sections with small thickness;

$$\Delta C_{Li} = C_{li}c_i / (MAC) = \frac{\{ (dC_l/d\alpha)_i \alpha_i + (C_{lo})_i \} c_i}{MAC}$$

$$C_L = 2 \int_0^{b/2} \Delta C_{Li} dy = 2 \sum_{i=1}^{i=k} 0.5 (\Delta C_{Li+1} + \Delta C_{Li}) (y_{i+1} - y_i)$$

For ideal lift loading in elliptical form;

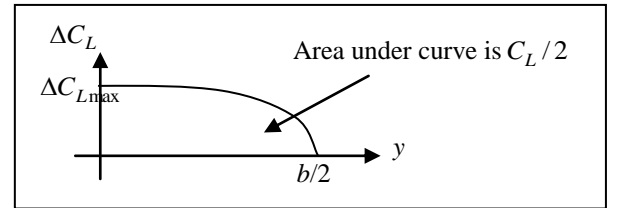


Figure 4: Elliptical lift loading

$$\frac{y_i^2}{(b/2)^2} + \frac{\Delta C_{Li}^2}{\Delta C_{L_{\max}}^2} = 1$$

Rearrange;

$$\Delta C_L = \left\{ \Delta C_{L_{\max}}^2 \left(1 - \frac{y^2}{(b/2)^2} \right) \right\}^{0.5}$$

Where $\Delta C_{L_{\max}}$ is local lift loading at centre section of the body and it is unknown.

$$C_L|_{\text{elliptic}} = \int_{y=0}^{y=b/2} \left\{ \Delta C_{L_{\max}}^2 \left(1 - \frac{y^2}{(b/2)^2} \right) \right\}^{0.5} dy$$

By equating $C_L|_{\text{elliptic}} = C_L$, $C_{L_{\max}}$ can be found. Local lift loading at each section can be calculated by;

$$\Delta C_{Li} = \left\{ \Delta C_{L\max}^2 \left(1 - \frac{y_i^2}{(b/2)^2} \right) \right\}^{0.5}$$

And local incidence angle can be found by;

$$\alpha_i = \frac{(\Delta C_{Li} MAC / c_i) - (C_{lo})_i}{(dC_l / d\alpha)_i}$$

Figure 5 below shows local lift loading, coefficients and ideal elliptical lift loading for Baseline-II BWB before inverse twist process. The loading at the body section is much larger than on the wing.

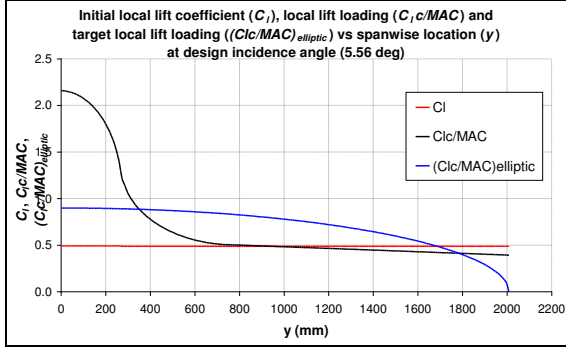


Figure 5: Local lift loading before inverse twist

By using equations mentioned before, the sectional incidence angle or twist angle is computed (Figure 6) to suit to elliptical lift loading and sectional lift coefficient (calculated based on local lift loading and local chord). Design trim angle is 5.56 degree at MAC spanwise location.

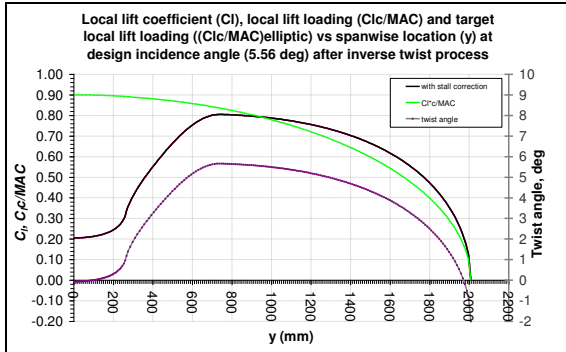


Figure 6: Lift loading and sectional twist angle after inverse twist process

Figure 7 shows the sectional airfoils after inverse twist process.

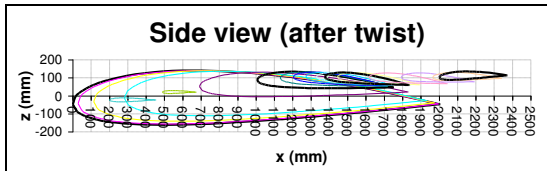


Figure 7: Side view after inverse twist process.

V. AERODYNAMICS

A CAD model is then created via CATIA and converted to machine language to produce a scale model made of aluminium by using CNC milling machine. The wind tunnel model is mounted on six-component balance mounting struts inside UiTM-LST wind tunnel. The test is conducted at Mach 0.1 or about 35 m/s with average air density of 1.17

kg/m³. The system uses DARCS3D data acquisition, control and noise reduction.

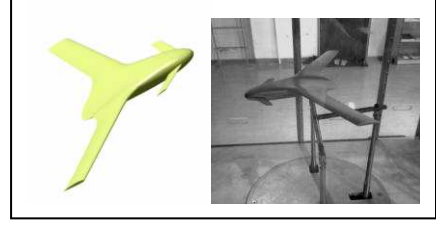


Figure 8: Baseline-II - from CAD to wind tunnel model.

Wind tunnel tests show vast improvement of lift coefficient on Baseline-II over Baseline-I (figure 9). The lift coefficient versus incidence angle ($C_L - \alpha$) for Baseline-II BWB above shows almost similar trend to Baseline-I (HANTU) BWB. Baseline-II possesses “lift dip” or reduction of lift at region of angle of attack from 8 to 12 degrees. Observation from the test suggests that the “dip” is caused by downwash from the canard to the wing especially at the tip the canard where tip vortex is produced (some sort of tornado at the tip of canard) that disrupt the potential flow around the wing span behind the canard.

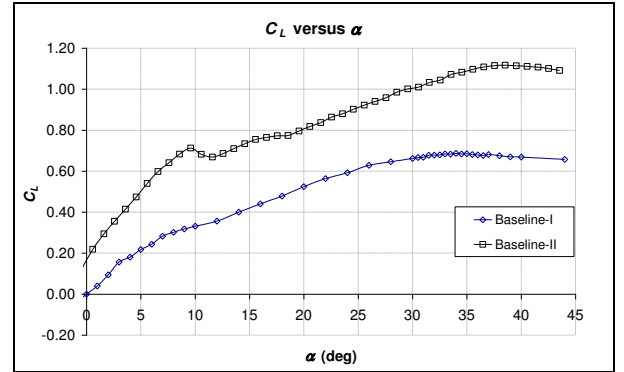


Figure 9: $C_L - \alpha$ curves

Continuation of lift increment at higher than 18 degrees incidence may be caused by a mixed of potential flow lift on the wing-body and leading edge vortex lift on the body alone. In this case, the trend is similar to Baseline-I BWB. Stall angle is around 37-38 degrees with maximum lift coefficient $C_{L\max}$ is around 1.15, 64 percent higher than Baseline-I's $C_{L\max}$. Baseline-II stalls at higher incidence angle than 35 degrees for Baseline-I. It also possesses higher lift at all incidence angles than Baseline-I with steeper change of lift w.r.t. incidence angle ($dC_L / d\alpha$) at low α and it is more linear than the old design. Summary of Baseline-II $C_L - \alpha$ relationship is given below;

Baseline-II: Low angle ($-5 < \alpha < 8$);

- Linear relationship; $C_L = 0.0636\alpha + 0.1787$
- Change of lift w.r.t. incidence angle;
 $\frac{dC_L}{d\alpha} = C_{L\alpha} = 0.0636$ per deg = 3.644 per rad
- Lift at zero incidence; $C_{L0} = 0.1787$
- Incidence angle at zero lift; $\alpha_{C_L=0} = -2.81$ deg
- Lift at 8 deg incidence; $C_L|_{\alpha=8} = 0.688$

High angle ($12 < \alpha < 32$)

- Linear relationship; $C_L = 0.0178\alpha + 0.4637$
- Change of lift w.r.t. incidence angle;
 $\frac{dC_L}{d\alpha} = C_{L\alpha} = 0.0178$ per deg = 1.020 per rad
- Lift at 12 deg incidence; $C_L|_{\alpha=12} = 0.677$
- Maximum lift; $C_{L_{\max}} = 1.15$
- Incidence angle at maximum lift; $\alpha_{C_{L_{\max}}} = 38.5$ deg

In short, Baseline-II's lift characteristic is better in all aspect than Baseline-I apart from lift dip due to canard factor.

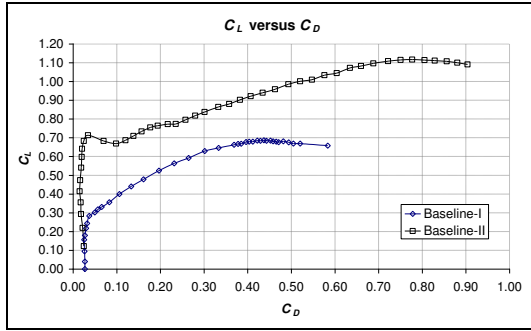


Figure 10: $C_L - C_D$ curves

Figure 10 shows relationships between lift and drag for both aircrafts. Baseline-I's curve resembles more parabolic curve than Baseline-II's curve which is "hectic" at medium lift region ($C_L = 0.6$ to 0.7), again, due to canard disturbance. However, Baseline-II can achieve lift coefficient of 0.7 at drag value very much lower than what Baseline-I can achieve at its maximum lift coefficient! At low incidence angle region, Baseline-II can utilize large lift without large drag penalty unlike its predecessor. At high incidence angle region, Baseline-II may have larger drag but it is also being supported by larger lift. In other words, this region is very useful for landing approach where large lift is needed for slower approach speed while large drag slows it down faster during touch down and ground roll.

The most useful region of lift-drag relationship is located at lower α region where the aircraft spends most of its time cruising and loitering. Zooming in to lower α region and swapping axis between lift and drag for easier parabolic regression (figure 11), one can see that Baseline-II has lower minimum drag than its predecessor does at 0.0157 versus 0.0250 – this is 37.2 percent reduction of drag!

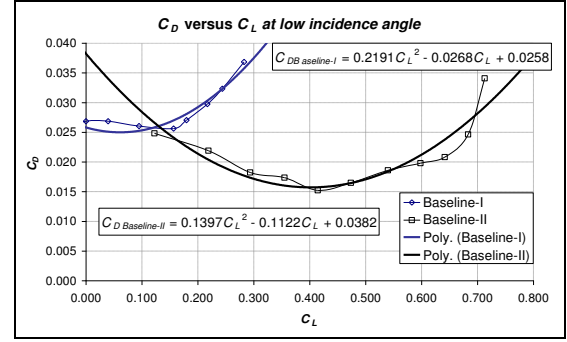


Figure 11: $C_D - C_L$ (zoom to lower α region)

Baseline-II's lift at minimum drag occurs at a more useful value of 0.4015 that correspond to about 3 degrees incidence angle rather than Baseline-I's 0.0612 which is slightly better than no lift at all. Baseline-I's wing is mid-mounted configuration making it less cambered than Baseline-II's high-wing configuration. As a result, drag at zero lift for Baseline-II is higher than Baseline-I at 0.0382 versus 0.0258 . This is no handicap for Baseline-II as minimum drag and lift-to-drag ratio that matter the most.

Low angle ($-5 < \alpha < 8$), low drag, low lift segment;

Baseline-II

- Parabolic relationship;
 $C_D = 0.1397C_L^2 - 0.1122C_L + 0.0382$
- Drag at zero lift, $C_{D0} = 0.0382$
- Lift at minimum drag, $C_L|_{D_{\min}} = 0.4015$
- Minimum drag, $C_{D_{\min}} = 0.0157$

Baseline-I

- Parabolic relationship;
 $C_D = 0.2191C_L^2 - 0.0268C_L + 0.0258$
- Drag at zero lift, $C_{D0} = 0.0258$
- Lift at minimum drag, $C_L|_{D_{\min}} = 0.0612$
- Minimum drag, $C_{D_{\min}} = 0.0250$

For the purpose of flight performance analysis, it is always convenient to look at lift-to-drag ratio to find its highest and its corresponding optimum lift and drag. Figure 12 compares $C_L / C_D - \alpha$ for Baseline-I and Baseline-II, and the graph shows almost unbelievable improvement by the latter over the former; 31 for the Baseline-II versus 8 for its predecessor, or even if Baseline-II wind tunnel test data is compared with Baseline-I's highest CFD data (that gives lower drag value than wind tunnel measurement due to more ideal environment) of 14. Perhaps the canard, which also acts like a small wing, helps in increasing lift while adding much smaller drag. The maximum L/D occurs at 5.9 degrees incidence for Baseline-II against 7 degrees incidence for Baseline-I. Baseline-II's incidence refers to incidence angle of mean aerodynamic chord of the wing-body and at this optimum reference incidence, the centre body incidence is at almost zero angle. Large body is at its lowest drag at zero incidence angle.

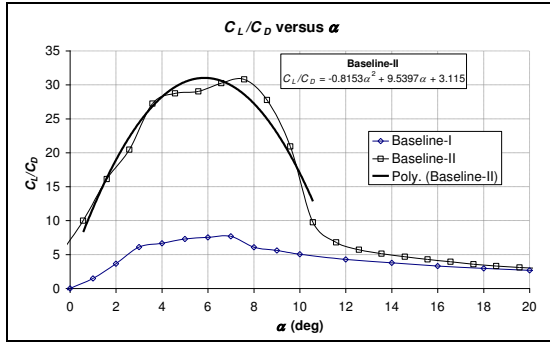


Figure 12: $C_L / C_D - \alpha$ (or lift-to-drag ratio, L/D versus incidence angle)

Baseline-I, however, has constant incidence angle at all spanwise station; be it the centre body, outer body or wing. Flying at 7 degrees incidence at mean aerodynamic chord means the whole body is also at the same incidence thus creates large drag. This explains why it has such a low L/D that it is worse than many conventional aircrafts' value and slightly better than Space Shuttle.

Baseline-II

- $(C_L / C_D)_{\max} = (L/D)_{\max} = 31$
- Optimum incidence; $\alpha_{(L/D)\max} = 5.9$ deg
- Optimum lift; $C_{L_{Opt}} = 0.560$
- Optimum drag; $C_{D_{Opt}} = 0.018$

Baseline-I

- $(C_L / C_D)_{\max} = (L/D)_{\max} = 8$
- Optimum incidence; $\alpha_{(L/D)\max} = 7.0$ deg
- Optimum lift; $C_{L_{Opt}} = 0.295$
- Optimum drag; $C_{D_{Opt}} = 0.037$

VI. FLIGHT PERFORMANCE ESTIMATION

Figure 13 is an example of performance estimation to evaluate the aerodynamics of both aircraft. Thrust required (TR) for steady-and-level flying aircraft is computed based on;

$$C_L = W / (0.5 \rho v^2 S) \dots (\text{similar weight and reference area})$$

$$C_D = f(C_L) \dots \text{refer to individual } C_D - C_L \text{ equations}$$

$$TR = D = 0.5 \rho v^2 S C_D$$

Where ρ and v is air density and airspeed, respectively. Weight and reference area are fixed for each aircraft and they are similar if one compares between Baseline-I and Baseline-II. As airspeed is varied, the value of C_L changes thus changing the C_D and, ultimately, TR . Minimum thrust required for Baseline-I at 111.6 kg weight is almost 135 N or 13.8 kg-f while Baseline-II at similar weight requires only 37 N or 3.8 kg-f of minimum thrust. Optimum cruising speed of Baseline-I is higher at Mach 0.17 but Baseline-II, with optimum cruising speed of Mach 0.11, is closer to cruising/loitering design airspeed.

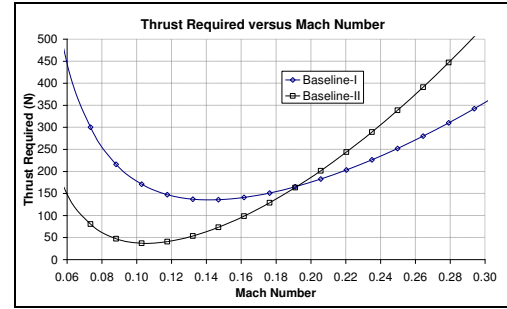


Figure 13: Thrust required versus Mach number

Baseline-II requires only 27.4 percent of thrust required by Baseline-I. This enables Baseline-II to cruise at much lower thrust setting or resort to smaller, lighter and lower-thrust rating engine – thus it is cheaper to run due to lower fuel consumption.

VII. CONCLUDING REMARKS

Planform modification or redesign with low-fidelity inverse twist method that give birth to Baseline-II BWB are able to solve shortcomings mentioned in early part of this paper. Large improvements are made to lift characteristic albeit with small snag at mid-range incidence angle due to flow disturbance on the wing by canard. Drag at cruising lift is further lowered causing staggering lift-to-drag ratio of 31. The effect of Baseline-II's $(L/D)_{\max}$ leap over the Baseline-I's reduces trust required at cruising speed to only 27.4 percent original required thrust of the latter. Baseline-II has been able to achieve its mission requirements at low-cost of fuel consumption.

ACKNOWLEDGMENT

Authors would like to express gratitude to the Ministry of Higher Education, Malaysia for funding the research through FRGS, Universiti Teknologi MARA through Dana Kecemerlangan Penyelidikan and Faculty of Mechanical Engineering, UiTM for upgrading FTTC wind tunnel facility.

REFERENCES

- [1] Liebeck RH, Page MA, Rawdon BK, "Blended Wing Body Subsonic Commercial Transport", AIAA Technical Paper 98-0438, (1998).
- [2] Engels, H., Becker, W., Morris, A. "Implementation of a multi-level methodology within the e-design of a blended wing body", Aerospace Science and Technology, 145-153 (2004).
- [3] Österheld C, Heinze W, Horst P., "Preliminary Design of A Blended Wing Body Configuration Using The Design Tool PrADO," Aerospace Science and Technology, 154-168 (2004)
- [4] D.W. Jung, M.H. Lowenberg. "Stability and control assessment of a blended-wing-body airliner configuration." AIAA Atmospheric Flight Mechanics Conference and Exhibition. San Francisco, California. 15-18 August 2005.
- [5] L. Bolsunovsky, N. P. Buzoverya, B. I. Gurvich, V. E. Denisov, A. I. Dunacvsky, L. M. Shkadov, O. V. Sonin, A. J. Udzhuhu, J. P. Zhurihin, "Flying Wing- Problems and Decisions", Aircraft Design 4,(2001). Pp. 193-219.
- [6] S. Saephan, C.P. Van Dam. "Simulation of the tumbling behaviour of tailless aircraft" 24Th Applied Aerodynamics Conference. San Francisco, California. 5-8 June 2008 (AIAA 2006-3321)
- [7] N. Qin, A. Vavalle, A. Le Moigne, M. Laban, K. Hackett, P. Weinertfelt, "Aerodynamic considerations of blended wing body aircraft," Progress in Aerospace Science (6), 321-343 (2004)
- [8] Z. Zhu, X. Wang, Z. Wu, Z. Chen. "A new type of transport: blended wing body aircraft." Hangkong Xuebao/Acta Aeronautica et Astronautica Sinica. Vol. 29. Issue 1. Jan. 2008. pp. 49-59.

- [9] Portsdam MA, Page MA, Liebeck RH, "Blended Wing Body Analysis and Design", AIAA Technical Paper 1997-2317, (1997).
- [10] J. Katz, S. Byre, R. Hahl. "Stall resistance features of lifting body airplane configurations." *Journal of aircraft*, No. 2, Vol. 36, 1999. pp. 471-478.
- [11] S. Wakayama, I Kroo, "The Challenge and Promise of Blended-Wing-Body Optimization", AIAA Technical Paper 2000-4740, (2000)
- [12] Roman D., Gilmore R. & Wakayama S. "Aerodynamics of high subsonic blended wing body configurations", AIAA Paper 2003-0554, (2003).
- [13] Liebeck RH, "Design of the Blended Wing Body Subsonic transport", *J Aircraft*. 41(1), 10-25 (2004).
- [14] Mamat, A.M., Nasir, R.E., Ngah, Z., Kuntjoro, W., Wisnoe, W., Ramly, R. "Aerodynamics of Blended Wing Body Unmanned Aerial Vehicle using Computational Fluid Dynamics". *Journal of Mechanical Engineering* 5 (2), 15-25, (2008).
- [15] H.V. de Castro. "Flying and handling qualities of a fly-by-wire blended-wing-body civil transport aircraft." PhD. Thesis. Cranfield University. (2003).
- [16] Wisnoe, W., Kuntjoro, W., Nasir, R.E., Mamat, A.M., Ramly, R. "Wind Tunnel Experiments of Blended Wing Body (BWB) Unmanned Aerial Vehicle (UAV) At Loitering Phase." *International Conference on Mechanical Engineering and Manufacturing* 2008, Johor Bahru. 21-23 May 2008.
- [17] Nasir, R.E., W., Wisnoe, Kuntjoro, W., Mamat, A.M. "The effect of centre elevator deflection on aerodynamics of Baseline-I blended wing body (BWB) unmanned aerial vehicle (UAV) developed in Universiti Teknologi MARA (UiTM) at low subsonic (Mach 0.3) using computational fluid dynamics." *International Conference on Advancement in Mechanical Engineering (ICAME)* 2009. Shah Alam, Malaysia (2009).
- [18] R. M. Cummings, S.A. Morton, S.G. Siegel. "Numerical prediction and wind tunnel experiment for a pitching unmanned combat air vehicle." *Aerospace Science and Technology* 12. (2008). PP. 355 – 364.
- [19] Nasir, R.E., Mamat, A.M., Ngah, Z., Kuntjoro, W., Wisnoe, W. "Aerodynamics of Blended Wing Body Unmanned Aerial Vehicle using Computational Fluid Dynamics at Mach 0.3". *Conference on Social & Scientific Research CSSR* 2006/2007. Sunway Lagoon Resort Hotel. 3-4th July 2007.
- [20] S. Siouris, N. Qin. "Study of the effects of wing sweep on the aerodynamic performance of a blended wing body aircraft." *Proceedings of Inst. Of Mech. Engineers*. Vol. 221. Part G: *Journal of Aerospace Engineering*. Pp. 47 – 55.